Effect of densimetric Froude number on local bridge pier scour

P. Williams, R. Balachandar & T. Bolisetti
University of Windsor, Windsor, Ontario, Canada

ABSTRACT: Over the past half-century, distress and collapse due to scour and scour-related complications have been shown to account for the majority of bridge failures in North America. Accordingly, there are several design standards which contain provisions for design of bridge piers with respect to scour on the basis of several design equations. These empirical equations have shown a tendency towards over-prediction of scour depth, which yields uneconomical design. Over the past several years, there have been a number of experimental investigations into local scour around bridge piers carried out at the University of Windsor with the intention of improving current scour depth estimation practices. While there is a large amount of scour modelling data publically available, there are many uncertainties regarding the conditions under which these tests were performed; hence, results of the present investigation were obtained under controllable conditions in order to isolate the effects of various non-dimensional quantities and attempt to quantify their individual and collective influences on scour depth and geometry. The focus of the majority of these investigations has been on determining effects of blockage ratio, flow shallowness (h/D), and relative coarseness (D/d_{50}) on maximum scour depth. Preliminary analysis indicated that D/d_{50} is of great importance in scour modelling, but variation in results indicated additional contributing parameters. Analysis of experimental results obtained indicated that an additional sediment-related non-dimensional parameter, the densimetric Froude number (F_d), also contributed to scour geometry.

1 INTRODUCTION

Due to a number of highly publicized bridge failures due to scour over the past several decades, there have been many investigations in recent years which have concluded that the majority of bridge failures in the United States have occurred as a result of scour or scour-related complications (Melville & Coleman 2000; Wardhana & Hadipriono 2003; Foti & Sabia 2011).

Such failures include the collapse of the Schoharie Creek bridge in upstate New York in 1987, in which unprecedented spring flooding caused failure of riprap protection around one of the bridge's piers, leading to collapse of three of its spans and the deaths of 10 motorists (LeBeau & Wadia-Fascetti 2007). Recently, similarly unanticipated flooding in June of 2013 resulted in the collapse of a Canadian Pacific railway bridge over the Bow River in Calgary, Alberta, derailing six train cars (CTV News 2013).

As a result of the prevalence and sudden nature of scour-induced bridge failures, several North American bridge design codes such as the AASHTO, the OHBDC, and the CHBDC include provisions for hydraulic design of bridge piers with respect to scour. This design is typically done on the basis of equilibrium scour depth (d_{se}) estimation, where d_{se} is the depth below which bridge pier foundations should be placed in order to avoid the effects of scouring action. The estimation of d_{se} is achieved using one of several code-specified "approved methods," which are empirical equations which have been derived experimentally.

While present understanding has improved and many such formulae are available, these methods often yield vastly different results, suggesting that there are aspects of scour which are still not well understood. Furthermore, the majority of commonly-used bridge pier scour depth estimation methods have a tendency to over-predict scour depth, yielding uneconomical design (Ettema et al. 1998).

2 LITERATURE REVIEW

Local scour is formed when a structure such as a bridge pier or abutment is introduced into a flow channel, inducing formation of several coherent turbulent structures in the flow field surrounding the pier (Figure 1). When fully-developed flow encoun-

ters the upstream face of an obstruction such as a bridge pier, its velocity abruptly becomes zero at a stagnation point, where pressure is also at a maximum. Flow velocity then increases along the streamline which leads from this stagnation point around the pier in the downstream direction (Figliola & Beasley 2011); this streamline then detaches from the pier once a certain velocity, known as separation velocity, is reached. It is at this point of separation where scouring action is induced and then progresses upstream until it reaches the upstream face of the pier (Guo 2012).

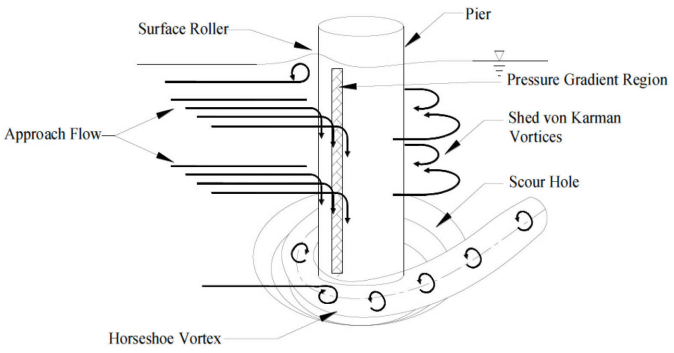

Figure 1. Depiction of the coherent turbulent structures in the flow field surrounding a bridge pier (Hodi 2009)

At the upstream face of the pier, there is a strong downward pressure gradient which induces formation of a vertical jet of water, known as the downflow (Dey et al. 1995). Once the downflow impinges upon the surface of the bed, it rolls up and around itself, extending in the downstream direction and forming what is known as the horseshoe vortex (named for its plan-view shape); this allows rapid removal of sediment to commence around the base of the pier (Melville & Coleman 2000). Wake vortices form due to flow around the pier and behave in such a way that mimics the motion of a tornado, removing sediment disturbed by the horseshoe vortex and depositing it downstream (Chiew 1984).

Scouring action due to these coherent turbulent flow structures continues until a state of equilibrium is reached, which is the point of time at which the strength of the horseshoe vortex is no longer capable of sediment removal from the bottom of the scour hole (Chiew 1984). If d_{se} is not reached until after the pier foundations have been exposed or, in extreme cases, undermined, then failure of the foundation is likely to occur (Ettema et al. 2011). Therefore, accurate estimation of d_{se} is of great importance with respect to serviceability in bridges.

Through dimensional analysis of scour-influencing parameters, the variables on which d_{se} relies most heavily can be reduced to in Equation 1. The majority of scour depth estimation methods are a function of any number of these variables.

$$d_{se} = f\{\rho, \nu, U, U_c, h, \rho_s, d_{50}, \sigma_g, g, D, Sh, Al\} \quad (1)$$

where, ρ = fluid density, ν = kinematic viscosity, U = mean flow velocity, U_c = critical velocity of sediment, h = mean flow depth, ρ_s = sediment density, d_{50} = median sediment diameter, σ_g = standard deviation of particle size, g = gravitational acceleration, D = pier width normal to the flow, Sh and Al = parameters describing pier shape and alignment.

When d_{se} is normalised with pier diameter D, this set of variables is condensed to a group of non-dimensional parameters, shown in Equation 2.

$$d_{se}/D = f\{U/U_c, h/D, D/d_{50}, Fr, Re, Sh, Al, \sigma_g\} \quad (2)$$

Equation 2 can be further reduced to Equation 3, contingent on maintenance of subcritical Froude number, sufficiently high Reynolds number, constant pier shape and alignment, and normally distributed sediment. Investigations have determined that relative scour depth (d_{se}/D) is, indeed, often a function of the three non-dimensional parameters shown in Equation 3 (flow intensity, U/U_c; flow shallowness, h/D; and relative coarseness, D/d_{50}).

$$d_{se}/D = f\{U/U_c, h/D, D/d_{50}\} \quad (3)$$

The relationship between relative scour depth and relative coarseness was investigated by Lee & Sturm in 2009. Experimental data from various investigations indicated that d_{se}/D increases with increasing D/d_{50} until a $D/d_{50} = 25$. After this point, d_{se}/D was shown to decrease with increasing D/d_{50} until D/d_{50} of approximately 200, after which point d_{se}/D was shown to be constant (Lee & Sturm 2009).

This relationship is of particular importance when considering that an inability to properly scale d_{50} is the principal differentiating factor between a laboratory model and a field prototype. In order to avoid scale effects in a hydraulic model such as those used in scour studies, geometric similitude must exist between the model and prototype (Heller 2011). While many length scales (D, h, etc.) can be scaled with reasonable accuracy in the model, if sediment size were to be scaled in the same manner, it would be of such size that it would be characterized as cohesive matter. In effect, in maintaining geometric similitude, flow-sediment interactions in the laboratory would differ greatly from those in the field. As a result, prototype-sized sediment is typically used in the model, and its values of D/d_{50} are comparably small. As described above, this would result in inaccurately deep scour in the model, which contributes to the previously-mentioned propensity of experimentally-developed equations to yield unnecessarily high estimates of scour. Further investigation into the nature and negligibility of such scale effects is therefore necessary in order to improve the effectiveness of current design practices (Ettema et al. 1998, 2011).

3 EXPERIMENTAL METHODOLOGY

Experimentation was conducted in the Ed Lumley Centre for Engineering Innovation's Sedimentation and Scour Study Laboratory at the University of Windsor in Ontario, Canada. The experiments were conducted in a horizontal flume with a length of 10.5 m, a width of 1.22 m, and a height of 0.84 m (Figure 2). A flow straightener, constructed from layers of pipe (d = 0.5 in) and secured with silicone, was placed at the upstream end of the flume in order to regulate the flow. A plywood approach ramp was constructed in order to allow flow progression to a plywood box which held the required bed sediment. The pump flow controller was calibrated using a V-notch weir at the downstream end of the flume.

Two non-cohesive sediments with d_{50} = 0.51 mm and 0.77 mm were used for experimentation; the standard deviation of particle size ($\sigma_g = \sqrt{d_{84}/d_{16}}$) of each was 1.16 and 1.34, respectively. The sieve analyses indicated that the sediments were uniformly distributed. For each test, channel blockage ratio (D/b = 10%), flow shallowness (h/D = 1.6), and flow intensity (U/U_c = 0.85) were held constant, such that the only varying non-dimensional parameter was relative coarseness. Flow intensity was held below unity, as the investigation dealt only with clear-water scour. Flow shallowness was maintained above 1.4 in order to ensure that piers were classified as narrow (Melville and Coleman 2000). The purpose of this experimentation was to isolate the effects of D/d_{50} on scour depth. Test parameters for experimentation are shown in Table 1.

It was determined through experimentation that there was a negligible difference in equilibrium depth of scour (d_{se}) in tests with run times of 72 hours and 48 hours. Therefore, 48 hours was deemed an acceptable length of testing time for the purposes of this investigation. For each test series, the appropriate sand was placed in the box inside the flume.

Following this, the walls were positioned in the sand bed such that the desired flume width was achieved (Figure 3). Once the walls were in place, the bed material was levelled using a flat trowel to ensure a level control surface. A model pier was then centered between the walls at a minimum distance of 1 meter downstream from the leading edge of the sand bed. Finally, the flume was filled to the desired water depth, the pump was turned on and brought up to a frequency necessary to sustain a flow intensity of 0.85.

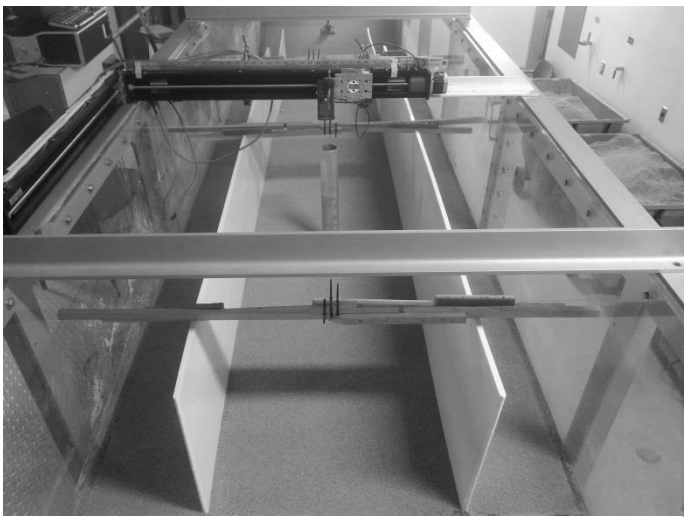

Figure 2. Experimental set-up at the Ed Lumley Centre for Engineering Innovation at the University of Windsor in Ontario, Canada

Table 1. Test conditions for experimentation

Test ID	D (m)	d_{50} (mm)	h (m)	b (m)	U (m/s)	Fr	D/d_{50}
A4	0.079	0.51	0.127	0.80	0.224	0.200	156
A5	0.070	0.51	0.112	0.71	0.224	0.213	137
A6	0.060	0.51	0.096	0.61	0.224	0.230	118
B1	0.121	0.77	0.193	1.22	0.259	0.188	157
B2	0.101	0.77	0.161	1.02	0.259	0.206	131
B3	0.089	0.77	0.142	0.90	0.259	0.219	115

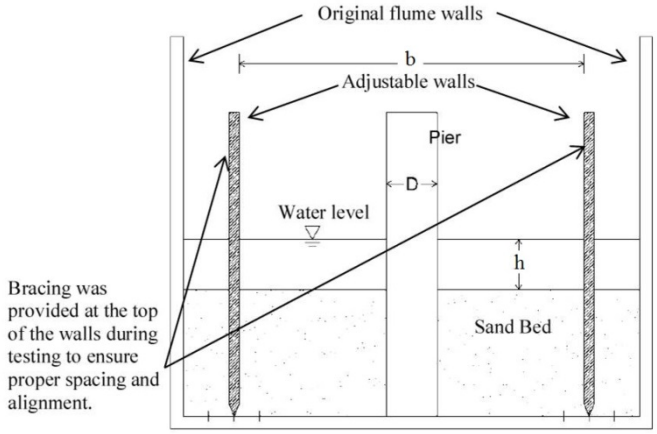

Figure 3. Schematic drawing of flume cross-section (D'Alessandro 2013)

The depth-averaged velocity of the approach flow, U, was verified for each test using an Acoustic Doppler Velocimeter (ADV, Nortek USA); point measurements were taken at 0.2 and 0.8 of the total water depth and then averaged in order to determine U. This test was then left to run for 48 hours. Once the run time had elapsed, the pump frequency was gradually brought down and then shut off. The flume was then drained such that flow emptied in a downstream direction, in order to avoid displacement of bed material. Once the flume was completely drained, the centreline and contour profiles of the scour hole were measured using a Leica laser distance meter mounted on a biaxial traverse.

Table 2. Summary of experimental results

est ID	d_{50} (mm)	d_{se} (cm)	d_{se}/D	w_s (cm)	w_s/D	Fr	D/d_{50}
A4	0.51	6.43	0.810	32.7	4.12	0.200	156
A5	0.51	6.23	0.892	32.2	4.61	0.213	137
A6	0.51	5.87	0.974	29.4	4.88	0.230	118
B1	0.77	7.51	0.622	43.4	3.60	0.188	157
B2	0.77	8.18	0.812	43.5	4.32	0.206	131
B3	0.77	7.26	0.817	37.9	4.26	0.219	115

4 RESULTS AND DISCUSSION

The results of testing are shown in Table 2, including equilibrium scour depth (d_{se}), relative scour depth (d_{se}/D), width of scour hole (w_s), and relative width of scour hole (w_s/D). Tests A4, A5 and A6 were conducted using bed material with a mean diameter of 0.51 mm, and test B1, B2, and B3 were conducted using bed material with d_{50} = 0.77 mm. For each test, pier diameter D was changed. Flume width b and water height h were scaled based on this changing D, in order to maintain constant flow shallowness (h/D) and blockage (D/b). Thus, the only varying primary non-dimensional parameter in each series of 3 test (series A and series B) was relative coarseness (D/d_{50}).

The dimensionless centreline and contour scour profiles for tests A4 through A6 are shown in Figures 4 and 6, respectively, and profiles for tests B1 through B3 are shown in Figures 5 and 7. The origin for each profile is located at the geometric centre of the pier. The x-axis is in the direction of flow, the y-axis is transverse to the flow, and the z-axis is normal to the x and y axes. Figures 4 and 5 demonstrate that tests with varying D/d_{50} and constant h/D, D/b, and U/U_c yield similar scour profiles. All tests with d_{50} = 0.77 mm resulted in scour profiles with primary sediment deposits downstream of the pier, and the lengths of these deposits were all less than five pier diameters (5D). Here, the deposit length refers to the distance between the first two points at which the centreline profile crosses the x-axis. Primary sediment deposits for all tests with d_{50} = 0.51 mm were longer than 5D; in addition, these deposits all consisted of bed formations in the form of ripples, which is common in sediment finer than 0.70 mm.

While the influences of D/d_{50} on scour geometry upstream of the pier were found to be small physically and quantitatively (Table 2, Figs 4-5), the downstream section of each centreline profile showed greater changes for tests with varying values of D/d_{50}. This is illustrated in Figure 6, where the relative scour depth at the downstream face of the pier generally increases with decreasing D/d_{50}.

As with the centreline profiles for the A and B tests, Figures 6 and 7 show that, in tests with varying D/d_{50} and all other primary non-dimensional parameters held constant, contour profiles are similar. However, this cannot be said of tests with different values of d_{50}. In Figure 6, scour for tests A4 through A6 (d_{50} = 0.51 mm) reached the sidewalls of the channel, indicating that despite a constant blockage ratio, secondary currents due to wall interference affected scouring. However, Figure 7 shows that for tests B1 through B3 (d_{50} = 0.77 mm), none of the scour profiles extended to the sidewalls. Therefore, scour in beds with finer sediment are more greatly affected by wall interference. For tests A4 through A6, scour generally reached the sidewalls at a lesser distance downstream of the pier for greater values of D/d_{50}. Therefore, if all other non-dimensional parameters of importance are constant between series A and series B, it follows that blockage influences must increase with sediment size, or some additional sediment-related parameter.

Figures 4 through 7 show that maximum scour depth and scour width both decrease with increasing D/d_{50} values, confirming the influence of D/d_{50} on scour depth described by Lee and Sturm (2009). This relationship between d_{se}/D and D/d_{50} is clearly shown by the results in series A and series B when each series is viewed separately. Between series A and series B, there are pairs of tests with very similar values of D/d_{50}; for example, B3 with D/d_{50} = 115 and A6 with D/d_{50} = 118, B2 with D/d_{50} = 131 and A5 with D/d_{50} = 137, or B1 with D/d_{50} = 157 and A4 with D/d_{50} = 156. Among these tests, all other primary non-dimensional parameters (h/D, U/U_c, etc.) are constant. Therefore, if D/d_{50} were indeed the only remaining non-dimensional parameter of influence, then it would follow that pairs of tests with such close values of D/d_{50} should have values of d_{se}/D that are also very close in magnitude and scour profiles that are nearly identical.

Comparison of profiles from each pair of tests in Figures 8 and 9 indicates that changes exist in d_{se}/D and w_s/D between tests of different sediment size, despite near-constant D/d_{50}. This indicates, again, that there is another sediment-related parameter which influences scour; through further analysis of results, this was determined to be the densimetric Froude number, F_d. Defined in Equation 4, the densimetric Froude number is representative of the ratio between the inertial force on each bed particle and its submerged specific weight (Hodi, 2009).

$$F_d = U/\sqrt{[g(SG-1)d_{50}]} \quad (4)$$

As previously discussed, the contour profiles of all series A tests in these comparative figures show that scouring action reached the sidewalls which, again, did not occur for any of the corresponding series B tests; this confirms that blockage effects are variable with changing d_{50} and therefore F_d. For tests in series A (d_{50} = 0.51 mm), F_d was calculated to be 2.40. For tests in series B (d_{50} = 0.77 mm), F_d was calculated to be 2.30. Therefore, the effects of wall interference from blockage increase with increasing F_d. Furthermore, when all other non-dimensional parameters are held constant, d_{se}/D decreases with decreasing F_d.

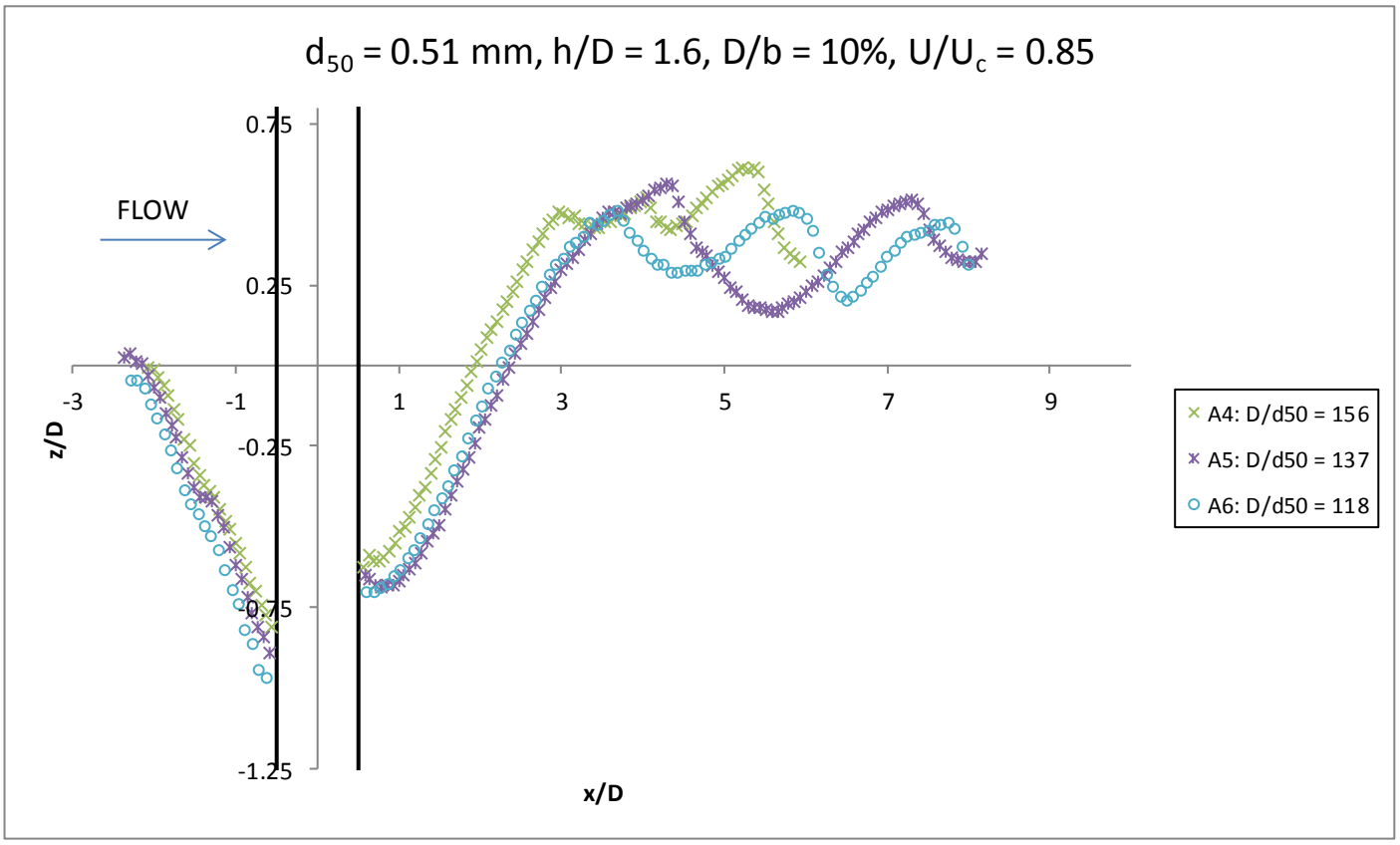

Figure 4. Centreline profiles for tests A4 through A6 (d_{50} = 0.51 mm with constant h/D, D/b, and U/U_c)

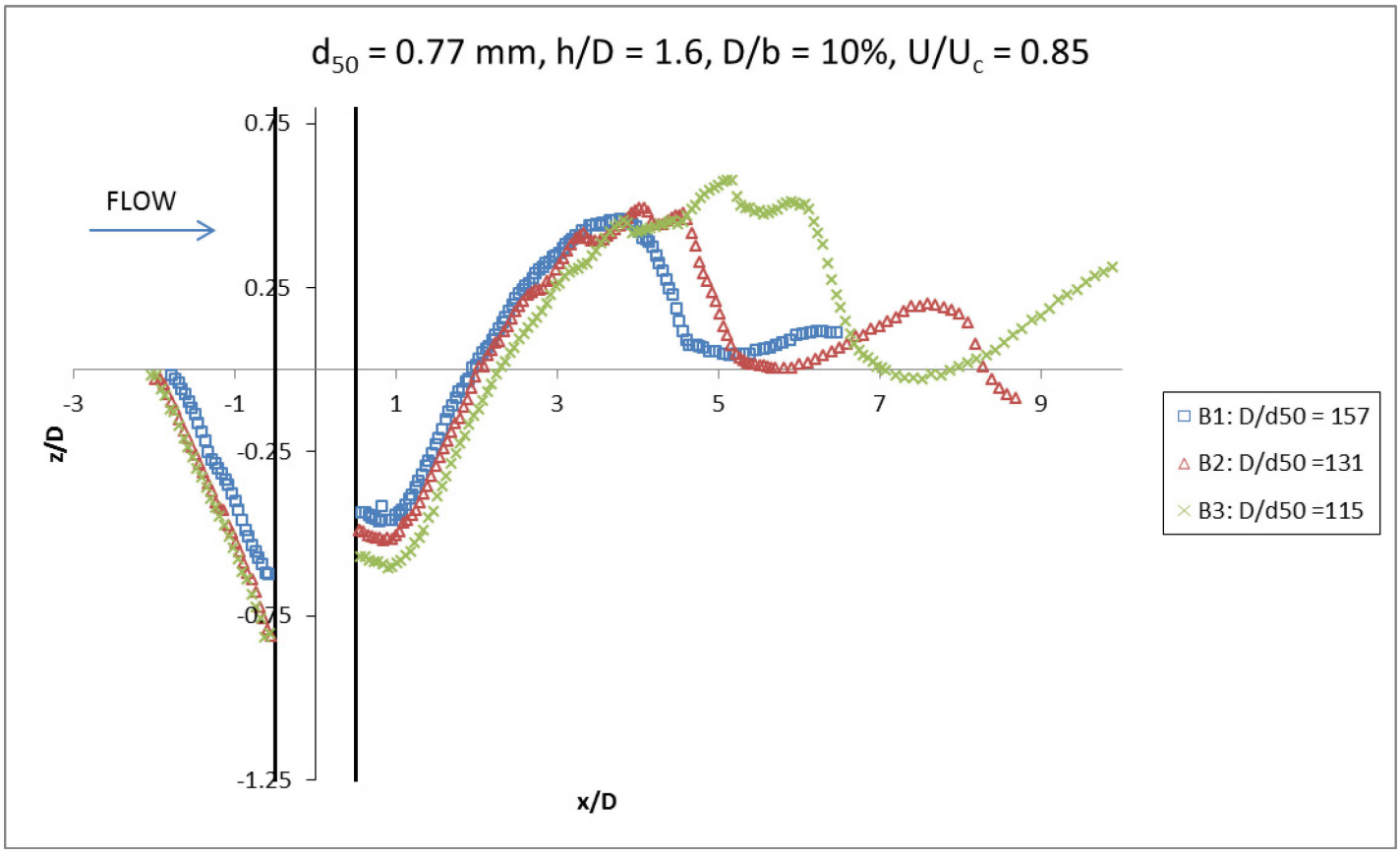

Figure 5. Centreline profiles for tests B1 through B3 (d_{50} = 0.77 mm with constant h/D, D/b, and U/U_c)

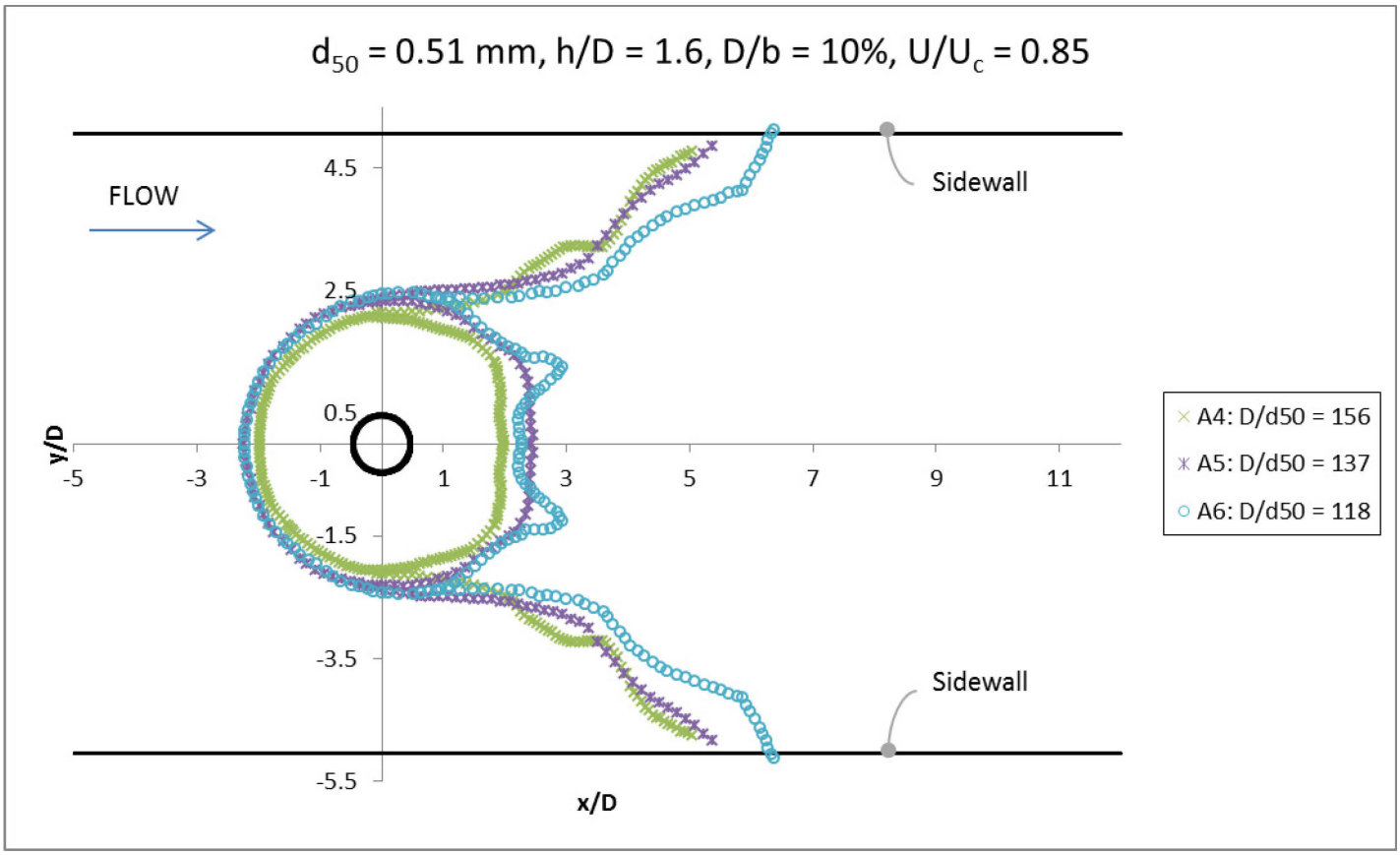

Figure 6. Contour profiles for tests A4 through A6 (d_{50} = 0.51 mm with constant h/D, D/b, and U/U_c)

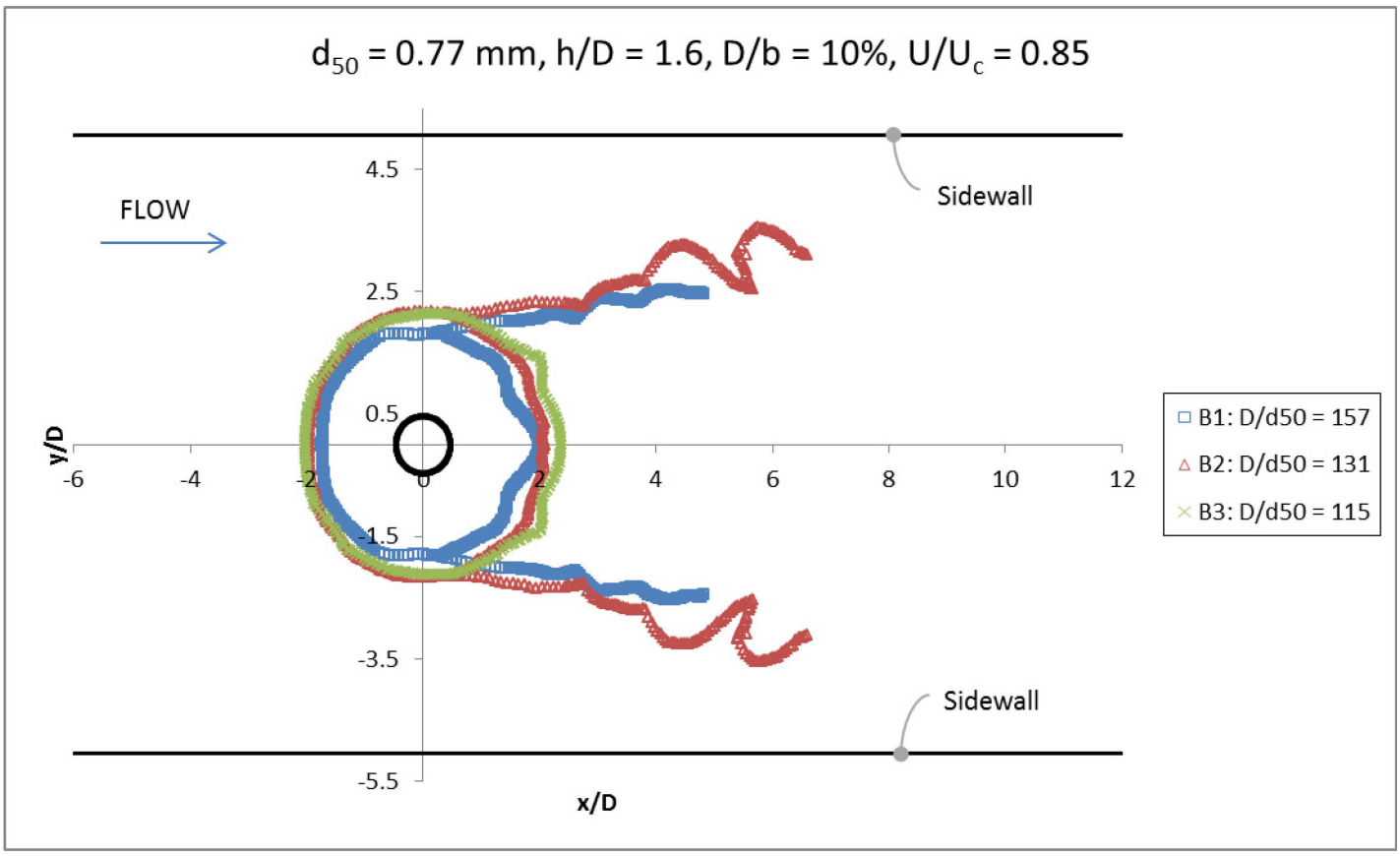

Figure 7. Contour profiles for tests B1 through B3 (d_{50} = 0.77 mm with constant h/D, D/b, and U/U_c)

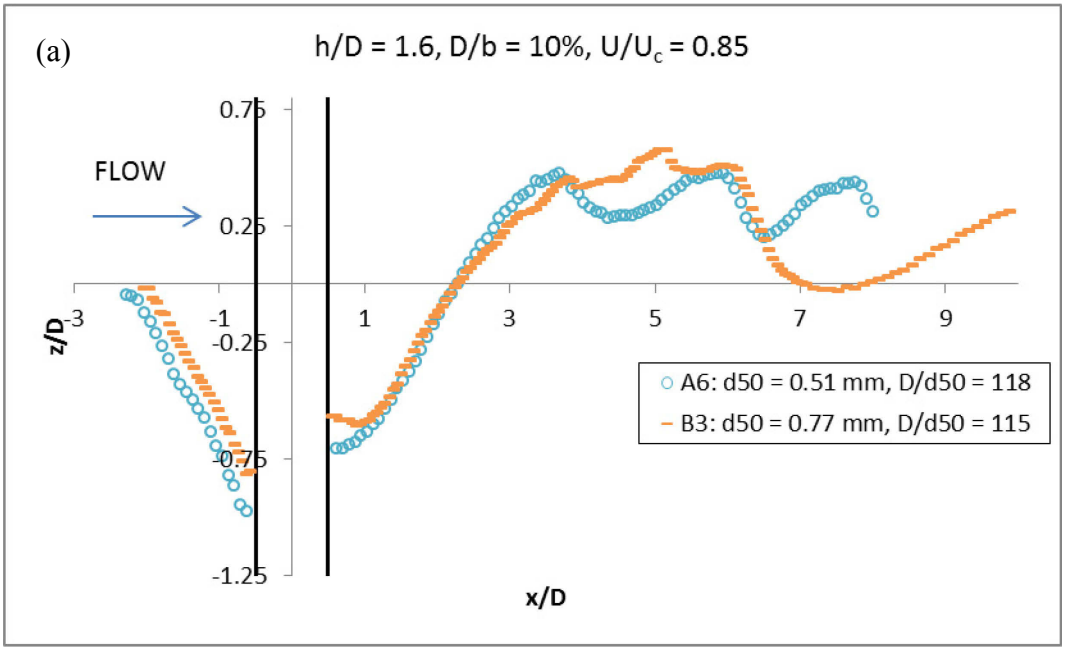

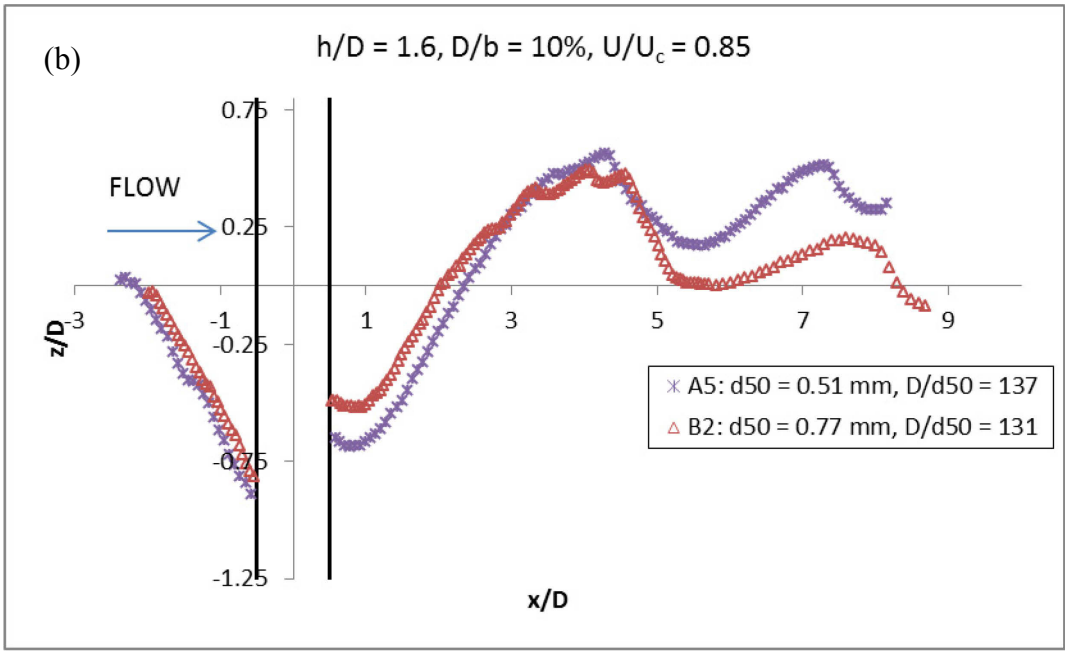

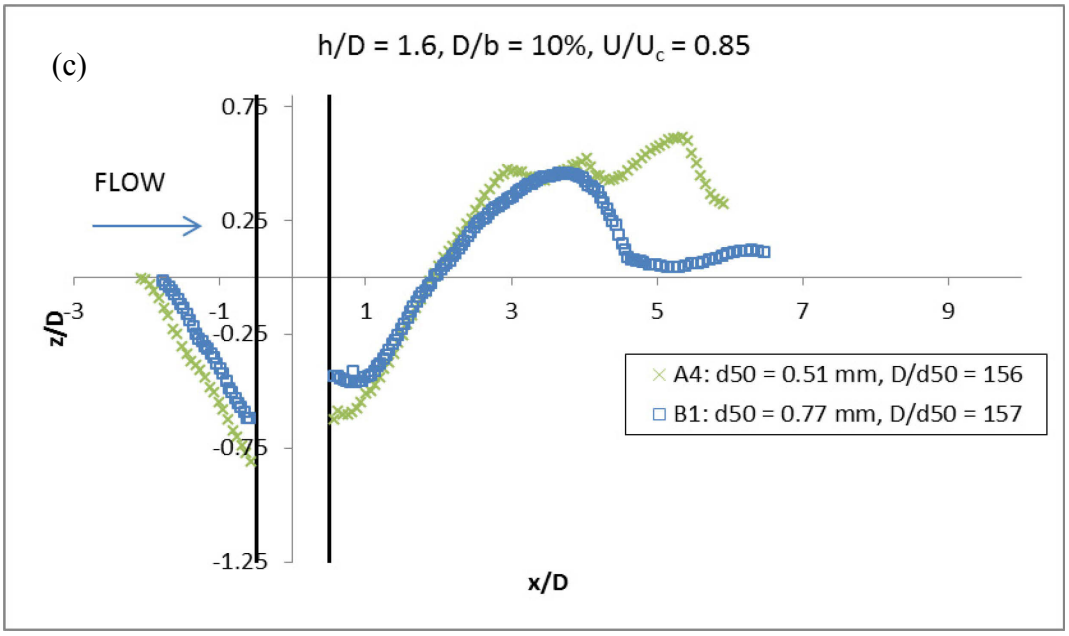

Figure 8. Comparison of centreline profiles for (a) tests A6 and B3, (b) tests A5 and B2 and (c) tests A4 and B1

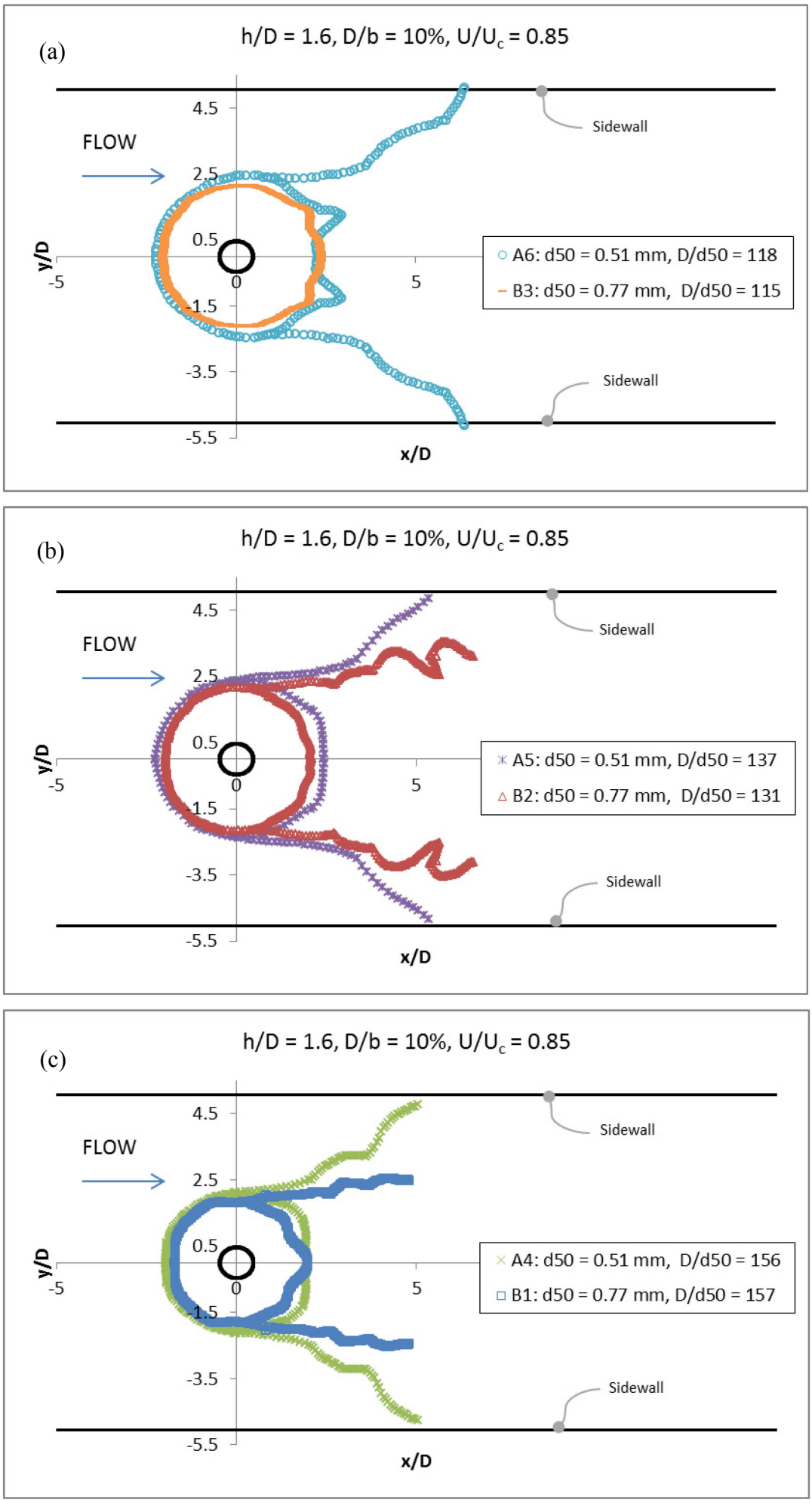

Figure 9. Comparison of contour profiles for (a) tests A6 and B3, (b) tests A5 and B2 and (c) tests A4 and B1

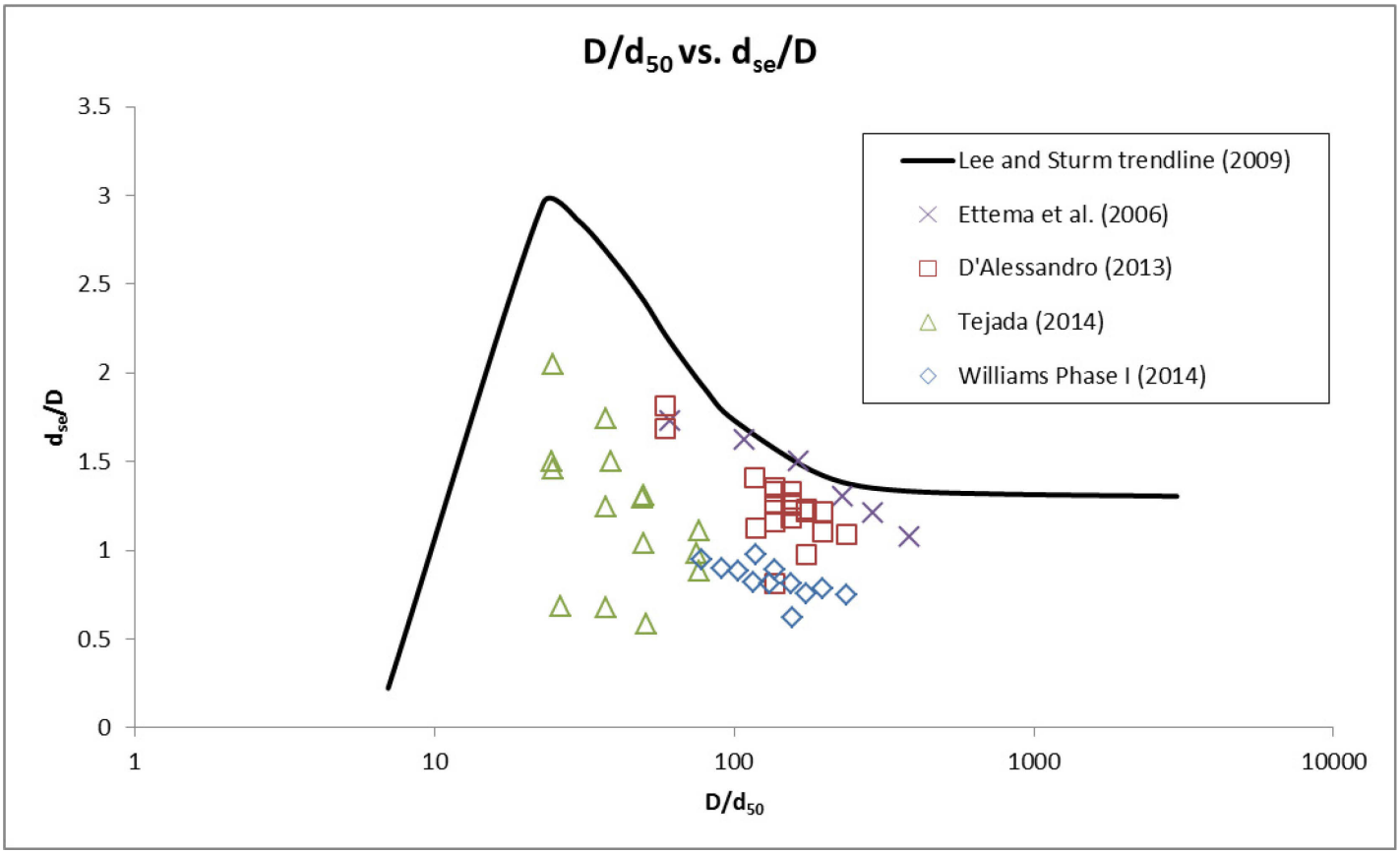

Figure 10. Variation of relative scour depth with relative coarseness for experimental results with D'Alessandro (2013), Tejada (2014), and Ettema et al. (2006)

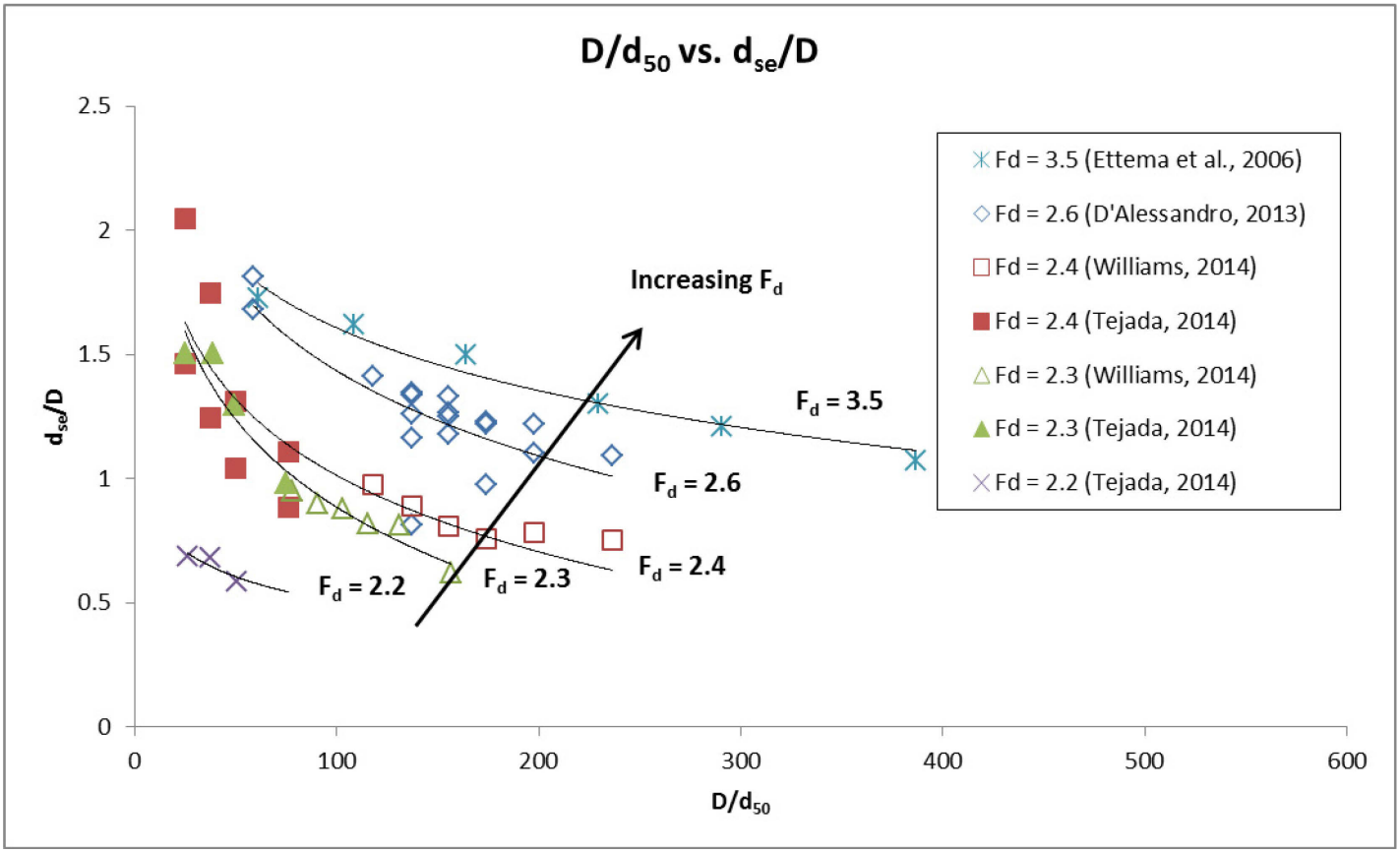

Figure 11. Variation of relative scour depth with relative coarseness grouped by densimetric Froude number for experimental results with D'Alessandro (2013), Tejada (2014), and Ettema et al. (2006)

Figure 10 shows the graphical relationship between d_{se}/D and D/d_{50} for several University of Windsor investigations (including series A and series B from the present study), as well as results from a study by Ettema et al. in 2006. The figure shows that while there is a decreasing trend between the two parameters, there is no distinct single curve upon which the data can be collapsed. There is a large amount of scatter in the relationship, which implies that there are other influencing parameters.

However, when grouped by values of densimetric Froude number, F_d (Fig. 11), a trend tends to appear. At least part of the scatter in the data can be attributed to varying values of F_d, with d_{se}/D decreasing with even small changes in F_d. Since F_d is representative of flow-sediment interactions, it was chosen as a primary parameter for estimation of relative scour depth. Therefore, the relationship between d_{se}/D and F_d can be determined in terms of D/d_{50}, which indicates that while D/d_{50} may not be the only governing parameter of highest influence, it still has an influence on d_{se}/D, particularly when compared with other non-dimensional quantities.

5 CONCLUSIONS AND RECOMMENDATIONS

In conclusion, it has been determined that d_{se}/D decreases with increasing D/d_{50}, which is in agreement with Lee & Sturm's (2009) trendline. In addition, the densimetric Froude number (representative of flow-sediment interactions) has been shown to affect d_{se}/D. Despite constant flow intensity and flow shallowness and near-constant relative coarseness, changes in scour depth and geometry were still demonstrate for tests in different sediment size. This indicated that another sediment-related non-dimensional parameter was had an effect on scour.

After analysis of experimental results from the present study, combined with previous experimental results from the University of Windsor and Ettema et al. (2006), it was determined that densimetric Froude number, F_d, was responsible for part of the discrepancies in scour depth and geometry between tests with similar values of U/U_c, h/D, and D/d_{50}.

It is recommended that further analysis be performed on experimental results in order to determine the feasibility of incorporation of F_d into scour depth estimation methods. The majority of scour depth estimation methods that are commonly used in current practice are experimentally-derived empirical functions of such non-dimensional parameters, and have a tendency to yield conservative estimates of scour depth, which leads to uneconomical design. Further experimentation on the influences of other governing non-dimensional parameters on scour is also recommended.

REFERENCES

American Association of State Highway and Transportation Officials. 2012. AASHTO LRFD Bridge Design Specifications. *American Association of State and Highway Transportation Officials*, Washington, D.C.

Chiew, Y. 1984. Local Scour at Bridge Piers. Ph.D Thesis, Auckland: School of Engineering, University of Auckland, New Zealand.

CSA International, Standards Council of Canada. 2006. Canadian Highway Bridge Design Code, CAN/CSA-26-06. *Canadian Standards Association*, Toronto, ON.

CTV News. 2013, June 27. *Calgary bridge failure caused by flooding*. CTV News. Retrieved February 28, 2014, from www.ctvnews.ca.

D'Alessandro, C. 2013. Effect of Blockage on Circular Bridge Pier Local Scour. M.A.Sc. Thesis, Faculty of Engineering, University of Windsor, Canada.

Dey, S., Bose, S., and Sastry, G. 1995. Clear Water Scour at Circular Piers: a Model. *Journal of Hydraulic Engineering*, 121(12), 869–876.

Ettema, R., Melville, B., and Barkdoll, B. 1998. Scale Effects in Pier-Scour Experiments. *Journal of Hydraulic Engineering*, 124(6), 639–642.

Ettema, R., Kirkil, G., and Muste, M. 2006. Similitude of Large-Scale Turbulence in Experiments on Local Scour at Cylinders. *Journal of Hydraulic Engineering*, 132(1), 33–40.

Figliola, R.S. and Beasley, D.E. 2011. *Theory and Design for Mechanical Measurements: Fifth Edition*. USA: John Wiley & Sons, Inc.

Foti, S. and Sabia, D. 2011. Influence of Foundation Scour on the Dynamic Response of an Existing Bridge. *J. Bridge Eng.*, 16(2), 295–304.

Guo, J. 2012. Pier Scour in Clear Water for Sediment Mixtures. *Journal of Hydraulic Research*, 50(1), 18-27.

Heller, V. 2011. Scale Effects in Physical Hydraulic Engineering Models. *Journal of Hydraulic Research*, 49(3), 293-306.

Hodi, B. 2009. Effect of Blockage and Densimetric Froude Number on Circular Bridge Pier Scour. M.A.Sc. Thesis, Faculty of Engineering, University of Windsor, Canada.

LeBeau, K. and Wadia-Fascetti, S. 2007. Fault Tree Analysis of Schoharie Creek Bridge Collapse. *J. Perform. Constr. Facil.*, 21(4), 320–326.

Lee, S. and Sturm, T. 2009. Effect of Sediment Size Scaling on Physical Modeling of Bridge Pier Scour. *Journal of Hydraulic Engineering*, 135(10), 793–802.

Melville, B., and Coleman, S. 2000. *Bridge Scour*. Colorado: Water Resources Publications.

Ettema, R., Melville, B., and Barkdoll, B. 1998. Scale Effects in Pier-Scour Experiments. *Journal of Hydraulic Engineering*, 124(6), 639–642.

Ettema, R., Constantinescu, G., Melville, B. 2011. NCHRP Web-Only Document 175: Evaluation of Bridge Scour Research: Pier Scour Processes and Predictions. From [http://onlinepubs.trb.org/onlinepubs/nchrp/nchrp_w175.pdf]

Ontario Ministry of Transportation, Quality and Standards Division (1991). Ontario Highway Bridge Design Code, 3rd edition. *Ontario Ministry of Transportation, Quality and Standards Division*, Toronto, ON.

Tejada, S. 2013. Effects of Blockage and Relative Coarseness on Clear Water Bridge Scour. M.A.Sc. Thesis, Faculty of Engineering, University of Windsor, Canada

Wardhana, K. and Hadipriono, F. 2003. Analysis of Recent Bridge Failures in the United States. *J. Perform. Constr. Facil.*, 17(3), 144–150.